

Precision Higgs Boson Probe of Type-II Seesaw Models

Saiyad Ashanujjaman^{1,2,*}, P. S. Bhupal Dev^{3,†}, Jihong Huang^{4,5,‡} and Shun Zhou^{4,5,§}

¹*Institut für Theoretische Teilchenphysik, Karlsruhe Institute of Technology, Engesserstraße 7, D-76128 Karlsruhe, Germany*

²*Institut für Astroteilchenphysik, Karlsruhe Institute of Technology, Hermann-von-Helmholtz-Platz 1, D-76344 Eggenstein-Leopoldshafen, Germany*

³*Department of Physics and McDonnell Center for the Space Sciences, Washington University, Saint Louis, MO 63130, USA*

⁴*Institute of High Energy Physics, Chinese Academy of Sciences, Beijing 100049, China*

⁵*School of Physical Sciences, University of Chinese Academy of Sciences, Beijing 100049, China*

Despite direct searches at the LHC excluding tripletlike Higgs bosons up to several hundred GeV over much of the type-II seesaw model parameter space, parts of it—most notably those featuring “cascade decays” of the charged Higgs bosons into their neutral partners and off-shell W bosons—still remain unconstrained. Meanwhile, measurements of the diphoton signal strength of the Standard Model (SM) Higgs boson—potentially modified by loop contributions from tripletlike Higgs states—are in good agreement with the SM expectation, with combined experimental uncertainties currently at approximately 8%. Given the trend in previous measurements, it is expected that future precision Higgs measurements at the HL-LHC and a future lepton collider such as the Circular Electron Positron Collider, Future Circular Collider, or Muon Collider will be consistent with the standard diphoton signal strength, albeit with significantly reduced uncertainties, down to about 0.7%. Presuming this and considering all relevant constraints, we explore whether such increasingly precise diphoton measurements can indirectly probe the parameter space that currently evades direct searches. We find that subpercent-level determinations of the diphoton rate will decisively probe a substantial fraction of this otherwise elusive region.

I. INTRODUCTION

The observation of nonzero neutrino masses and mixing provides a strong impetus for going beyond the Standard Model (SM). A particularly elegant resolution is provided by the Weinberg operator-induced seesaw mechanism [1]. Among its three canonical ultraviolet completions [2], the type-II seesaw model [3–8], which augments the SM with an $SU(2)_L$ -triplet scalar field carrying hypercharge $Y = 2$, has attracted considerable interest due to its distinctive phenomenological signatures and potential testability at current and future colliders [9–83] (for reviews, see Refs. [84, 85]), as well as at low-energy experiments [50, 54, 55, 86–89]. This model introduces several new Higgs bosons, namely, the doubly charged ($H^{\pm\pm}$), singly charged (H^\pm), and CP -even and CP -odd neutral (H^0 and A^0) Higgs bosons. Direct searches at the LEP and LHC experiments have put stringent constraints on these new scalars. LEP experiments (OPAL and DELPHI) have set a lower-mass limit of about 100 GeV for $H^{\pm\pm}$ decaying into $\ell^\pm\ell^\pm$ ($\ell = e, \mu$) [90, 91]. For H^\pm decaying into cs or $\tau\nu$, a lower limit of about 80 GeV has been set by ALEPH, DELPHI, L3, and OPAL [92]. The OPAL experiment also placed a limit of 55 GeV on the neutral scalar states H^0 and A^0 decaying into $\nu\bar{\nu}$ [12]. At the LHC, the ATLAS Collaboration has set a lower limit of 1020 GeV for $H^{\pm\pm}$ decaying into $\ell^\pm\ell^\pm$ [93–95],

while CMS has placed a limit of 535 GeV for decays exclusively into $\tau^\pm\tau^\pm$ [96]. Also, ATLAS has excluded $H^{\pm\pm}$ decaying into $W^\pm W^\pm$ in the 200–350 GeV mass range [97].¹

Broadly speaking, the phenomenology, and hence the exclusion limits, of the type-II seesaw model depends on three parameters: the doubly charged Higgs mass $m_{H^{\pm\pm}}$, the mass splitting $\Delta m = m_{H^{\pm\pm}} - m_{H^\pm}$, and the triplet vacuum expectation value (VEV) v_Δ [20, 27, 68]. The regions with $\Delta m \lesssim \mathcal{O}(1)$ GeV are dominated by the “golden decays” of $H^{\pm\pm}$ to $\ell^\pm\ell^\pm$ (or $W^\pm W^\pm$) for v_Δ smaller (or larger) than $\mathcal{O}(0.1)$ MeV, and therefore are highly constrained by the experimental searches mentioned above. In contrast, the region with larger $\Delta m \gtrsim \mathcal{O}(1)$ GeV is dominated by the “cascade decays” of $H^{\pm\pm}$ and H^\pm to H^0/A^0 and off-shell W -bosons, with H^0/A^0 subsequently decaying into $\nu\bar{\nu}$ or $b\bar{b}, t\bar{t}, ZZ, Zh, hh$ depending on v_Δ . The presence of off-shell W bosons and multiple decay steps leads to soft visible objects, missing energy, and large SM backgrounds, rendering conventional LHC searches ineffective. Consequently, this region remains largely unconstrained by direct searches to date [68, 70, 78]. Moreover, low-mass $H^{\pm\pm}$ (84–200 GeV) decaying into $W^\pm W^\pm$ are yet to be excluded [41, 74]. In this Letter, we show for the first time, to the best of our knowledge, that indirect probes—such as precision measurements of the SM Higgs boson properties at the LHC and future lepton colliders like Circular Electron Positron Collider (CEPC), Future Circular Collider (FCC-ee) or

* saiyad.ashanujjaman@kit.edu

† bdev@wustl.edu

‡ huangjh@ihep.ac.cn

§ zhoush@ihep.ac.cn

¹ Ref. [68] has estimated an improved exclusion range of 200–400 GeV by reinterpreting some of these LHC searches.

MuC—could provide a powerful complementary handle on this otherwise elusive region of parameter space.

In particular, the new charged Higgs bosons H^\pm and $H^{\pm\pm}$, if relatively light, can significantly contribute to the loop-induced SM Higgs decay into diphotons, $h \rightarrow \gamma\gamma$ [33, 36, 45, 98]. This, in turn, imposes nontrivial constraints on regions of the model parameter space that would otherwise evade direct searches. Notably, the LHC measurements of the corresponding signal strength $\mu_{h \rightarrow \gamma\gamma}$ are in good agreement with the SM prediction [99–101], with the current experimental uncertainty of approximately 10% [102, 103], down to about 8% when combined with the Tevatron data [104]. Even though recent determinations lie somewhat above the SM expectation, the pattern of past measurements suggests that upcoming results from the HL-LHC [105], and a future lepton collider such as CEPC [106], FCC-ee [107], or MuC [108], will likely consolidate the SM prediction for the SM Higgs-to-diphoton signal strength, albeit with significantly improved precision—potentially reducing uncertainties to as low as 1.3% (0.7%) when combining HL-LHC measurements with those from CEPC or FCC-ee (MuC) [109, 110]. Presuming such a scenario, and taking into account all relevant constraints, we explore in this Letter how future precision measurements of the Higgs diphoton signal could provide a complementary probe of the hitherto unconstrained elusive regions of the type-II seesaw model parameter space.

II. THE MODEL AND CURRENT CONSTRAINTS

In the type-II seesaw model [3–8], the SM is augmented with an $SU(2)_L$ -triplet scalar field with $Y = 2$:

$$\Delta = \begin{pmatrix} \Delta^+/\sqrt{2} & \Delta^{++} \\ \Delta^0 & -\Delta^+/\sqrt{2} \end{pmatrix}. \quad (1)$$

The most general scalar potential is given by

$$\begin{aligned} V = & -m_\Phi^2 \Phi^\dagger \Phi + \frac{\lambda}{4} (\Phi^\dagger \Phi)^2 + m_\Delta^2 \text{Tr}(\Delta^\dagger \Delta) \\ & + [\mu (\Phi^T i\sigma^2 \Delta^\dagger \Phi) + \text{H.c.}] + \lambda_1 (\Phi^\dagger \Phi) \text{Tr}(\Delta^\dagger \Delta) \\ & + \lambda_2 [\text{Tr}(\Delta^\dagger \Delta)]^2 + \lambda_3 \text{Tr}[(\Delta^\dagger \Delta)^2] + \lambda_4 \Phi^\dagger \Delta \Delta^\dagger \Phi, \end{aligned} \quad (2)$$

where Φ is the SM Higgs doublet; m_Φ^2, m_Δ^2 and μ are the mass parameters, and λ and λ_i ($i = 1, \dots, 4$) are the dimensionless quartic couplings. The neutral components of Φ and Δ procure respective VEVs $v_\Phi/\sqrt{2}$ and $v_\Delta/\sqrt{2}$, satisfying $\sqrt{v_\Phi^2 + 2v_\Delta^2} = v \approx 246$ GeV. For a detailed description of the scalar potential and its dynamical features, see Ref. [29]. The electroweak symmetry breaking gives rise to several physical states: two CP -even states (h and H^0), two CP -odd states (G^0 and A^0), two singly charged states (G^\pm and H^\pm), and a doubly charged state $H^{\pm\pm}$. Here, G^0 and G^\pm are the *would-be* Nambu-Goldstone bosons, and h is identified as

the 125 GeV Higgs boson observed at the LHC. All the scalar potential parameters can be traded in terms of the physical masses $m_h, m_{H^0}, m_{A^0}, m_{H^\pm}, m_{H^{\pm\pm}}$, the VEVs v_Φ, v_Δ , and the rotation angle α of the CP -even Higgs states [29]. For $v_\Delta^2 \ll v_\Phi^2$ (as required by electroweak precision constraints, see below), the tripletlike Higgs states follow the sum rule

$$m_{H^{\pm\pm}}^2 - m_{H^\pm}^2 \approx m_{H^\pm}^2 - m_{H^0/A^0}^2 \approx -\frac{\lambda_4}{4} v_\Phi^2. \quad (3)$$

The model also features a Yukawa interaction term with the SM lepton doublet:

$$-\mathcal{L}_{\text{int}} \supset Y_{\alpha\beta} L_\alpha^T C i \sigma^2 \Delta L_\beta + \text{H.c.}, \quad (4)$$

where C is the charge conjugation matrix, σ^2 is the second Pauli matrix, and (α, β) denote the lepton flavor index. This Yukawa term, together with the μ -term in the scalar potential, breaks lepton number when Δ acquires a VEV, thereby generating tree-level Majorana neutrino masses:

$$m_\nu = \sqrt{2} Y v_\Delta. \quad (5)$$

The tripletlike Higgs bosons can decay either into a pair of SM particles or into a lighter triplet partner accompanied by an off-shell W/Z boson. In broad terms, these decays can be categorized into three classes: (i) leptonic decays, (ii) diboson decays, and (iii) cascade decays, in which the parent Higgs decays into a lighter partner and an off-shell W/Z boson. The branching ratios for these decay modes are highly sensitive to two key parameters: the mass splitting $\Delta m = m_{H^{\pm\pm}} - m_{H^\pm}$ and the triplet VEV v_Δ (see, for instance, Ref. [68]). In Fig. 1, we present the decay phase diagram of tripletlike Higgs bosons (see also Ref. [26]), illustrating regions where different decay categories dominate in the v_Δ - Δm parameter space. For definiteness, we show only the case of the doubly charged Higgs boson $H^{\pm\pm}$ with a mass of 400 GeV. Similar decay patterns are observed for the other tripletlike Higgs states, though these are not shown for brevity.

As discussed in Sec. I, the parameter space dominated by cascade decays of $H^{\pm\pm}$ and H^\pm to H^0/A^0 plus off-shell W bosons—depicted in blue in Fig. 1—remains largely unconstrained by the direct searches thus far; see Fig. 2 for a summary of the current exclusion limit on $m_{H^{\pm\pm}}$ in the v_Δ - Δm plane. In what follows, we briefly outline the relevant constraints on the model:

- i) *Theoretical constraints:* Tree-level perturbative unitarity and boundedness-from-below conditions on the scalar couplings restrict the theoretically viable parameter space within the perturbative regime. These constraints have been extensively studied; see, e.g., Refs. [29, 33, 35].
- ii) *Lepton flavor violation:* The Yukawa interaction (4) leads to flavor-changing lepton decays such as $\mu \rightarrow e\gamma$, $\mu \rightarrow eee$, and muonium-antimuonium oscillation. This also results in enhanced contributions

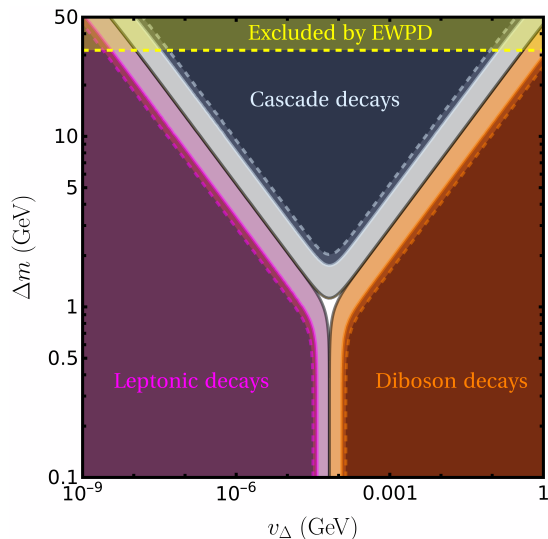


FIG. 1. Decay phase diagram of the doubly charged Higgs bosons in the v_Δ - Δm parameter space. Dashed (solid) contours in magenta, orange, and light blue represent 95% (90%) branching ratios, while black solid contours indicate 50% branching ratios for the corresponding decay modes. The region shown in blue remains unconstrained by the direct searches thus far. For definiteness, we set $m_{H^{\pm\pm}} = 400$ GeV. The yellow-shaded region above the dashed horizontal line is excluded by the current EWPD at 95% CL. For the other tripletlike Higgs states, the decay phase diagrams are qualitatively similar. For the $\Delta m < 0$ scenario, the region with $\Delta m \lesssim -40$ GeV is excluded by EWPD.

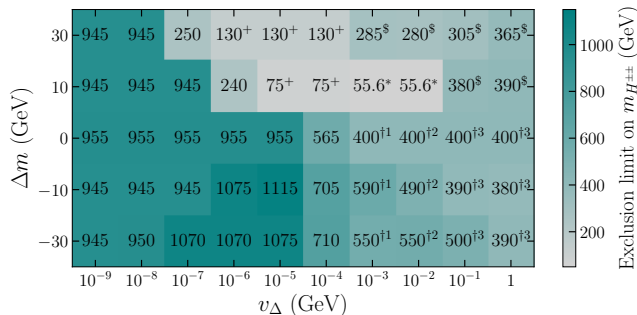


FIG. 2. Estimated 95% CL lower limits on $m_{H^{\pm\pm}}$ in the v_Δ - Δm parameter space. Entries marked with superscript ‘†1’, ‘†2’ [‘†3’] and ‘\$’ respectively denote region where masses of 150–200 (95–200) [80–200] GeV and 55.6–200 GeV are not excluded yet; those with a superscript ‘+’ (‘*’) refer to limits derived from LEP monophoton searches (Z -pole width bound on $Z \rightarrow H^+H^-$).

to $e^-e^+ \rightarrow \ell^-\ell^+$ cross sections. Upper limits on these processes, combined with neutrino oscillation data, impose a *lower* bound on $v_\Delta \gtrsim \mathcal{O}(\text{eV})$ for $m_{H^{\pm\pm}} \sim \mathcal{O}(\text{TeV})$ [53, 54, 86–88]. The exact limit depends on the lightest neutrino mass and the mass hierarchy.

iii) Collider Limits: In Fig. 2, we summarize the lim-

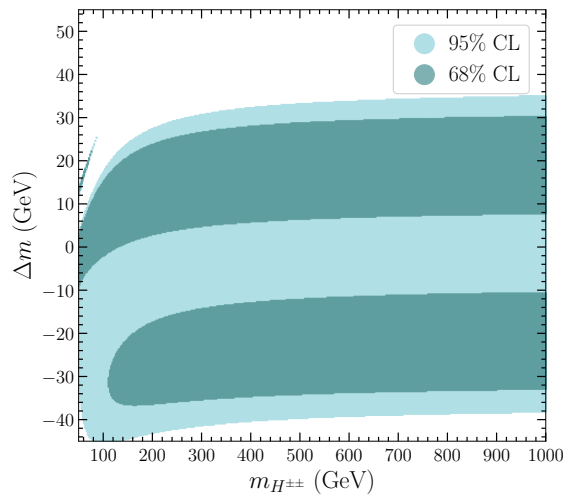


FIG. 3. Region of the parameter space allowed by the EWPD (taken from PDG [113]) at 68% and 95% CL in the $m_{H^{\pm\pm}}$ - Δm plane.

its from collider searches in the v_Δ - Δm parameter space. The entries indicate the 95% CL lower limits on $m_{H^{\pm\pm}}$, as obtained in Refs. [12, 68, 93]. Entries marked with superscripts ‘†1’ (‘†2’) [‘†3’] and ‘\$’ respectively denote regions where masses of 150–200 (95–200) [80–200] GeV and 55.6–200 GeV are not yet excluded. Those with a superscript ‘+’ (‘*’) refer to limits derived from monophoton searches (Z -pole width bound on $Z \rightarrow H^+H^-$) at LEP [12]. In regions where H^\pm decays to $\ell^\pm\nu$ or $\tau\nu$, limits from slepton searches at LEP and the LHC, lepton universality in W decays from LEP, as well as from τ decay lifetime and universality are relevant; however, direct searches targeting $H^{\pm\pm} \rightarrow \ell^\pm\ell^\pm$ provide stronger limits.

iv) Electroweak Precision Data (EWPD): The new Higgs bosons contribute to gauge boson self-energies, affecting the EWPD. These effects are well captured by the oblique parameters S , T , and U at the one-loop level [111, 112]; see Supplemental Material for their expressions. Notably, the triplet Higgs bosons also modify the T parameter at tree level (or, rather, the ρ parameter): $\alpha_{\text{em}}T_{\text{tree}} \equiv \rho - 1 = -2v_\Delta^2/v^2$, where $\alpha_{\text{em}} = e^2/4\pi$ is the electromagnetic fine-structure constant. This gives an *upper* bound on $v_\Delta \lesssim \mathcal{O}(1)$ GeV, which justifies the limit $v_\Delta \ll v$ used in Eq. (3).

In Fig. 3, we present the region of the model parameter space consistent with the EWPD at 68% and 95% confidence level (CL) in the $m_{H^{\pm\pm}}$ - Δm plane. Here, we adopt the EWPD fit results from PDG 2024 [113].² We see that a mass splitting up to

² Currently, no global fit incorporates the latest ATLAS [114] and

about 30 (40) GeV is allowed for $\Delta m > (<)0$ by the EWPD. The corresponding excluded region is indicated by the yellow-shaded area in Fig. 1.

v) SM Higgs Signal Strength: The new Higgs bosons can significantly affect precision observables of the SM Higgs, particularly the global and diphoton signal strengths (the discussion of the latter is deferred to the next section). To a very good approximation, the global signal strength is just scaled by $\cos^2 \alpha$. By combining the Tevatron and LHC measurements, Ref. [104] estimates this value to be $\mu_{h,\text{global}} = 1.012 \pm 0.034$. This translates into a limit of $|\alpha| \lesssim 0.24$ (0.30) at 2σ (3σ).

III. HIGGS DIPHOTON SIGNAL STRENGTH

The inclusive diphoton signal strength of the SM Higgs boson is defined as

$$\mu_{h \rightarrow \gamma\gamma} = \frac{\sigma_h}{\sigma_h^{\text{SM}}} \times \frac{\Gamma_{h \rightarrow \gamma\gamma} / \Gamma_{h,\text{tot}}}{\Gamma_{h \rightarrow \gamma\gamma}^{\text{SM}} / \Gamma_{h,\text{tot}}^{\text{SM}}}, \quad (6)$$

where $\sigma_h / \sigma_h^{\text{SM}} \approx \cos^2 \alpha$ is the production cross section of h normalized to its SM value, and $\Gamma_{h,\text{tot}}$ is the total decay width of h with its SM value $\Gamma_{h,\text{tot}}^{\text{SM}} = (4.088 \pm 0.014)$ MeV at $m_h = 125$ GeV [117]. The loop-induced diphoton decay rate is given by [33, 36, 118]

$$\Gamma_{h \rightarrow \gamma\gamma}^{(\text{SM})} = \frac{\alpha_{\text{em}}^2 G_F m_h^3}{128 \sqrt{2} \pi^3} \left| g_{h\gamma\gamma}^{(\text{SM})} \right|^2, \quad (7)$$

where G_F is the Fermi coupling, α_{em} should be taken at the scale $q^2 = 0$ since the final state photons are real, and the effective couplings $g_{h\gamma\gamma}^{(\text{SM})}$ are given in the Supplemental Material.

To obtain the total decay width $\Gamma_{h,\text{tot}}$, one needs to compute all other decays of h in the present model. The decay rates for $f\bar{f}/gg$, WW , and ZZ modes can be obtained by scaling the corresponding SM decay rates with $(g_{ff}^h)^2$, $(g_{WW}^h)^2$, and $(g_{ZZ}^h)^2$. These couplings, normalized to their SM value, are given by

$$g_{ff}^h \approx \cos \alpha, \quad (8)$$

$$g_{WW}^h \approx \cos \alpha + \frac{2v\Delta}{v} \sin \alpha, \quad (9)$$

$$g_{ZZ}^h \approx \cos \alpha + \frac{4v\Delta}{v} \sin \alpha. \quad (10)$$

CMS [115] measurements of the W -boson mass. However, as these results are fully compatible with the PDG 2024 combination [113], we expect that their inclusion would lead to only a marginal shift in the best-fit values of S , T , and U , leaving the overall phenomenology largely unchanged. Further, in this work, we do not include the latest CDF result for the W -mass measurement [116]—which would have favored a larger Δm [69, 71–73]—since it has not been confirmed by the most recent measurements from ATLAS [114] and CMS [115].

The loop-induced $h \rightarrow Z\gamma$ decay also gets additional contributions from the triplet scalars [36, 119, 120] (see Supplemental Material) and this is properly taken into account in our numerical calculation. The current experimental uncertainty in the $h \rightarrow Z\gamma$ channel is $\sim 70\%$ [121], compared to the $\sim 8\%$ precision for $h \rightarrow \gamma\gamma$, making the diphoton channel the most powerful indirect probe at present. Future improvements in $h \rightarrow Z\gamma$ could provide a complementary handle.

IV. PRECISION DIPHOTON PROBE OF THE ELUSIVE PARAMETER SPACE

As noted earlier, the triplet Higgs parameter space where cascade decays of $H^{\pm\pm}$ and H^\pm into H^0/A^0 and off-shell W bosons are dominant (illustrated in blue in Fig. 1) remains beyond the reach of current direct search strategies. Also, the region with low-mass $H^{\pm\pm}$ (84–200 GeV) decaying into $W^\pm W^\pm$ is yet to be excluded [41, 74]. Figure 4 shows this direct-search-inaccessible parameter space currently *allowed* by theoretical constraints and EWPD at 95% CL, depicted as the light gray region in the background. We now assess the sensitivity of precision SM Higgs diphoton measurements to probe this region.

The hadron collider experiments at the Tevatron ($\sqrt{s} = 1.96$ TeV) and the LHC ($\sqrt{s} = 7, 8, \text{ and } 13$ TeV) have performed several measurements of the inclusive diphoton signal strength of the SM Higgs boson. A recent combined analysis of these measurements, presented in Ref. [104], reports a signal strength of 0.99 ± 0.04 for the combined Higgs production and 1.10 ± 0.07 for the combined $h \rightarrow \gamma\gamma$ decay. Consequently, from Eq. (6), the combined $\mu_{h \rightarrow \gamma\gamma}$ is

$$\mu_{h \rightarrow \gamma\gamma} = 1.09 \pm 0.08. \quad (11)$$

Here we analyze four benchmark scenarios reflecting different levels of precision in measuring $\mu_{h \rightarrow \gamma\gamma}$. The first scenario corresponds to the current global average (11), while the remaining three represent anticipated improvements from future measurements/experiments:

- i) Current:* $\mu_{h \rightarrow \gamma\gamma} = 1.09 \pm 0.08$ [104],
- ii) HL-LHC (optimistic):* $\mu_{h \rightarrow \gamma\gamma} = 1.00 \pm 0.019$ [109],
- iii) HL-LHC+FCC-ee/CEPC:* $\mu_{h \rightarrow \gamma\gamma} = 1.00 \pm 0.013$ [109],
- iv) HL-LHC+10 TeV MuC:* $\mu_{h \rightarrow \gamma\gamma} = 1.00 \pm 0.007$ [110].

Note that the central value for all future measurements is assumed to be consistent with the SM (which serves as a good reference point), while the precision of the future measurements is reflected in the error bar. We emphasize that the results presented in this work are driven primarily by the anticipated improvement in experimental precision, and are therefore robust against modest shifts in the assumed central value of $\mu_{h \rightarrow \gamma\gamma}$.

The resulting allowed regions in the model parameter space are shown in Fig. 4, where the model parameters

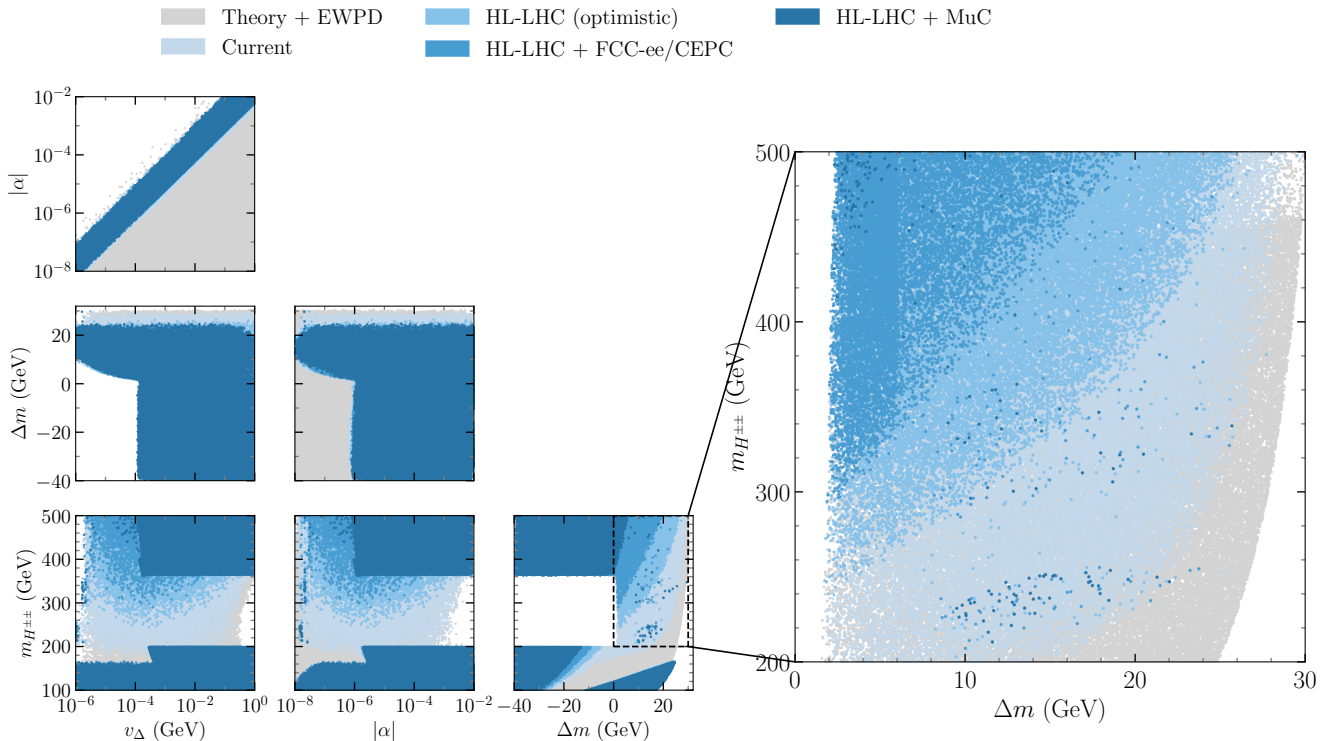


FIG. 4. Direct-search-inaccessible parameter space allowed by theoretical constraints and EWP at 95% CL (light gray). Overlaid regions in blue shades indicate the parameter space compatible with future $\mu_{h \rightarrow \gamma\gamma}$ measurements of increasing precision (darker blue represents higher precision). The enlarged panel on the right highlights the cascade-decay regime, characterized by the sequential decay $H^{\pm\pm} \rightarrow H^\pm \rightarrow H^0/A^0$, which can be almost completely probed by the expected precision to be achieved at a future MuC.

are varied in the ranges shown. The white regions are already ruled out. The currently allowed region is shown in light blue, while projected future sensitivities are illustrated with progressively darker shades of blue: light blue (HL-LHC optimistic), normal blue (HL-LHC + FCC-ee/CEPC), and dark blue (HL-LHC + 10 TeV MuC). The present constraint—driven by the $\approx 8\%$ experimental uncertainty—still permits a wide swath of parameter space that is inaccessible to direct searches, particularly in the cascade-dominated region characterized by the sequential decay $H^{\pm\pm} \rightarrow H^\pm \rightarrow H^0/A^0$ (see the enlarged panel of Fig. 4). However, the progressively darker shaded regions illustrate how rapidly this region shrinks once percent-level precision is achieved. Note also that throughout the allowed region one finds $|\alpha| \sim v_\Delta/v_\Phi$, i.e., α is typically two orders of magnitude smaller than the triplet VEV, reflecting the expected suppression of doublet-triplet mixing.

The HL-LHC (optimistic) scenario already removes a substantial portion of the parameter space, especially for larger $|\Delta m|$ or lighter $H^{\pm\pm}$, where the charged-scalar loop contributions tend to drive $\mu_{h \rightarrow \gamma\gamma}$ away from unity. Once subpercent precision is achieved—through the HL-LHC in combination with FCC-ee/CEPC or, in particular, with 10 TeV MuC—the surviving parameter space is further reduced. For the HL-LHC+FCC-ee/CEPC

projection, the allowed region becomes noticeably narrower, corresponding mainly to heavy or nearly degenerate triplet spectra. In contrast, for the HL-LHC+10 TeV MuC case, the viable points become sparse, surviving only as a few isolated points scattered throughout the plane.

V. SUMMARY AND OUTLOOK

We have examined the region of the type-II seesaw parameter space that remains unconstrained by current LHC searches. This “elusive” region, consistent with perturbative unitarity, vacuum stability, and electroweak precision data, extends to light tripletlike Higgs bosons and allows sizable mass splittings among them.

We showed that precision measurements of the Higgs diphoton signal strength, $\mu_{h \rightarrow \gamma\gamma}$, which gets loop contributions from the charged scalars H^\pm and $H^{\pm\pm}$, provides a sensitive indirect probe of this uncharted parameter space. Using the current global average and projected precisions from the HL-LHC, FCC-ee/CEPC, and 10 TeV MuC, we identified the parameter regions compatible with each scenario. While the present $\sim 8\%$ uncertainty leaves much of the direct-search-inaccessible space open, percent-level precision at the HL-LHC al-

ready removes a substantial portion of it. The subpercent level precision measurements anticipated at future lepton colliders further restrict the model: the HL-LHC+FCC-ee/CEPC projection favors relatively heavy or nearly degenerate triplet spectra, whereas the MuC leaves only a few isolated points surviving across the plane.

In summary, precision Higgs measurements offer a robust and complementary probe of the type-II seesaw mechanism. Future improvements in the Higgs-to-diphoton signal strength are poised to play a central role in extending the experimental sensitivity to the region inaccessible to direct searches.

ACKNOWLEDGMENTS

This research is supported by the Deutsche Forschungsgemeinschaft (DFG, German Research Foundation) under grant 396021762 - TRR 257, the National Natural Science Foundation of China under Grant No. 12475113, the CAS Project for Young Scientists in Basic Research (YSBR-099), and the Scientific and Technological Innovation Program of IHEP under Grant No. E55457U2. The work of B.D. was partly supported by the US Department of Energy under grant No. DE-SC0017987 and by a Humboldt Fellowship from the Alexander von Humboldt Foundation. B.D. thanks the Theory Group at IHEP, Beijing for warm hospitality where this work was initiated, and also thanks the Astroparticle Group at KIT for a seminar visit where part of this work was done.

REFERENCES

- [1] S. Weinberg, Baryon and Lepton Nonconserving Processes, *Phys. Rev. Lett.* **43**, 1566 (1979).
- [2] E. Ma, Pathways to naturally small neutrino masses, *Phys. Rev. Lett.* **81**, 1171 (1998), [arXiv:hep-ph/9805219](#).
- [3] W. Konetschny and W. Kummer, Nonconservation of Total Lepton Number with Scalar Bosons, *Phys. Lett. B* **70**, 433 (1977).
- [4] J. Schechter and J. W. F. Valle, Neutrino Masses in $SU(2) \times U(1)$ Theories, *Phys. Rev. D* **22**, 2227 (1980).
- [5] T. P. Cheng and L.-F. Li, Neutrino Masses, Mixings and Oscillations in $SU(2) \times U(1)$ Models of Electroweak Interactions, *Phys. Rev. D* **22**, 2860 (1980).
- [6] M. Magg and C. Wetterich, Neutrino Mass Problem and Gauge Hierarchy, *Phys. Lett. B* **94**, 61 (1980).
- [7] G. Lazarides, Q. Shafi, and C. Wetterich, Proton Lifetime and Fermion Masses in an $SO(10)$ Model, *Nucl. Phys. B* **181**, 287 (1981).
- [8] R. N. Mohapatra and G. Senjanovic, Neutrino Masses and Mixings in Gauge Models with Spontaneous Parity Violation, *Phys. Rev. D* **23**, 165 (1981).
- [9] K. Huitu, J. Maalampi, A. Pietila, and M. Raidal, Doubly charged Higgs at LHC, *Nucl. Phys. B* **487**, 27 (1997), [arXiv:hep-ph/9606311](#).
- [10] J. F. Gunion, C. Loomis, and K. T. Pitts, Searching for doubly charged Higgs bosons at future colliders, eConf **C960625**, LTH096 (1996), [arXiv:hep-ph/9610237](#).
- [11] S. Chakrabarti, D. Choudhury, R. M. Godbole, and B. Mukhopadhyaya, Observing doubly charged Higgs bosons in photon-photon collisions, *Phys. Lett. B* **434**, 347 (1998), [arXiv:hep-ph/9804297](#).
- [12] A. Datta and A. Raychaudhuri, Mass bounds for triplet scalars of the left-right symmetric model and their future detection prospects, *Phys. Rev. D* **62**, 055002 (2000), [arXiv:hep-ph/9905421](#).
- [13] M. Muhlleitner and M. Spira, A Note on doubly charged Higgs pair production at hadron colliders, *Phys. Rev. D* **68**, 117701 (2003), [arXiv:hep-ph/0305288](#).
- [14] E. J. Chun, K. Y. Lee, and S. C. Park, Testing Higgs triplet model and neutrino mass patterns, *Phys. Lett. B* **566**, 142 (2003), [arXiv:hep-ph/0304069](#).
- [15] A. G. Akeroyd and M. Aoki, Single and pair production of doubly charged Higgs bosons at hadron colliders, *Phys. Rev. D* **72**, 035011 (2005), [arXiv:hep-ph/0506176](#).
- [16] T. Han, B. Mukhopadhyaya, Z. Si, and K. Wang, Pair production of doubly-charged scalars: Neutrino mass constraints and signals at the LHC, *Phys. Rev. D* **76**, 075013 (2007), [arXiv:0706.0441 \[hep-ph\]](#).
- [17] J. Garayoa and T. Schwetz, Neutrino mass hierarchy and Majorana CP phases within the Higgs triplet model at the LHC, *JHEP* **03**, 009, [arXiv:0712.1453 \[hep-ph\]](#).
- [18] M. Kadastik, M. Raidal, and L. Rebane, Direct determination of neutrino mass parameters at future colliders, *Phys. Rev. D* **77**, 115023 (2008), [arXiv:0712.3912 \[hep-ph\]](#).
- [19] A. G. Akeroyd, M. Aoki, and H. Sugiyama, Probing Majorana Phases and Neutrino Mass Spectrum in the Higgs Triplet Model at the CERN LHC, *Phys. Rev. D* **77**, 075010 (2008), [arXiv:0712.4019 \[hep-ph\]](#).
- [20] P. Fileviez Perez, T. Han, G.-y. Huang, T. Li, and K. Wang, Neutrino Masses and the CERN LHC: Testing Type II Seesaw, *Phys. Rev. D* **78**, 015018 (2008), [arXiv:0805.3536 \[hep-ph\]](#).
- [21] F. del Aguila and J. A. Aguilar-Saavedra, Distinguishing seesaw models at LHC with multi-lepton signals, *Nucl. Phys. B* **813**, 22 (2009), [arXiv:0808.2468 \[hep-ph\]](#).
- [22] A. G. Akeroyd and C.-W. Chiang, Doubly charged Higgs bosons and three-lepton signatures in the Higgs Triplet Model, *Phys. Rev. D* **80**, 113010 (2009), [arXiv:0909.4419 \[hep-ph\]](#).
- [23] W. Rodejohann, Inverse Neutrino-less Double Beta Decay Revisited: Neutrinos, Higgs Triplets and a Muon Collider, *Phys. Rev. D* **81**, 114001 (2010), [arXiv:1005.2854 \[hep-ph\]](#).
- [24] A. G. Akeroyd, C.-W. Chiang, and N. Gaur, Leptonic signatures of doubly charged Higgs boson production at the LHC, *JHEP* **11**, 005, [arXiv:1009.2780 \[hep-ph\]](#).
- [25] W. Rodejohann and H. Zhang, Higgs triplets at like-sign linear colliders and neutrino mixing, *Phys. Rev. D* **83**, 073005 (2011), [arXiv:1011.3606 \[hep-ph\]](#).
- [26] A. Melfo, M. Nemevsek, F. Nesti, G. Senjanovic, and Y. Zhang, Type II Seesaw at LHC: The Roadmap, *Phys. Rev. D* **85**, 055018 (2012), [arXiv:1108.4416 \[hep-ph\]](#).
- [27] M. Aoki, S. Kanemura, and K. Yagyu, Testing the Higgs triplet model with the mass difference at the LHC, *Phys. Rev. D* **85**, 055007 (2012), [arXiv:1110.4625 \[hep-ph\]](#).
- [28] A. G. Akeroyd and H. Sugiyama, Production of doubly charged scalars from the decay of singly charged scalars

- in the Higgs Triplet Model, *Phys. Rev. D* **84**, 035010 (2011), [arXiv:1105.2209 \[hep-ph\]](#).
- [29] A. Arhrib, R. Benbrik, M. Chabab, G. Moultaqa, M. C. Peyranere, L. Rahili, and J. Ramadan, The Higgs Potential in the Type II Seesaw Model, *Phys. Rev. D* **84**, 095005 (2011), [arXiv:1105.1925 \[hep-ph\]](#).
- [30] A. G. Akeroyd, S. Moretti, and H. Sugiyama, Five-lepton and six-lepton signatures from production of neutral triplet scalars in the Higgs Triplet Model, *Phys. Rev. D* **85**, 055026 (2012), [arXiv:1201.5047 \[hep-ph\]](#).
- [31] C.-W. Chiang, T. Nomura, and K. Tsumura, Search for doubly charged Higgs bosons using the same-sign diboson mode at the LHC, *Phys. Rev. D* **85**, 095023 (2012), [arXiv:1202.2014 \[hep-ph\]](#).
- [32] E. J. Chun and P. Sharma, Same-Sign Tetra-Leptons from Type II Seesaw, *JHEP* **08**, 162, [arXiv:1206.6278 \[hep-ph\]](#).
- [33] E. J. Chun, H. M. Lee, and P. Sharma, Vacuum Stability, Perturbativity, EWPD and Higgs-to-diphoton rate in Type II Seesaw Models, *JHEP* **11**, 106, [arXiv:1209.1303 \[hep-ph\]](#).
- [34] M. Aoki, S. Kanemura, M. Kikuchi, and K. Yagyu, Radiative corrections to the Higgs boson couplings in the triplet model, *Phys. Rev. D* **87**, 015012 (2013), [arXiv:1211.6029 \[hep-ph\]](#).
- [35] F. Arbabifar, S. Bahrani, and M. Frank, Neutral Higgs Bosons in the Higgs Triplet Model with nontrivial mixing, *Phys. Rev. D* **87**, 015020 (2013), [arXiv:1211.6797 \[hep-ph\]](#).
- [36] P. S. B. Dev, D. K. Ghosh, N. Okada, and I. Saha, 125 GeV Higgs Boson and the Type-II Seesaw Model, *JHEP* **03**, 150, [Erratum: *JHEP* 05, 049 (2013)], [arXiv:1301.3453 \[hep-ph\]](#).
- [37] S. Kanemura, K. Yagyu, and H. Yokoya, First constraint on the mass of doubly-charged Higgs bosons in the same-sign diboson decay scenario at the LHC, *Phys. Lett. B* **726**, 316 (2013), [arXiv:1305.2383 \[hep-ph\]](#).
- [38] E. J. Chun and P. Sharma, Search for a doubly-charged boson in four lepton final states in type II seesaw, *Phys. Lett. B* **728**, 256 (2014), [arXiv:1309.6888 \[hep-ph\]](#).
- [39] F. del Águila and M. Chala, LHC bounds on Lepton Number Violation mediated by doubly and singly-charged scalars, *JHEP* **03**, 027, [arXiv:1311.1510 \[hep-ph\]](#).
- [40] Z. Kang, J. Li, T. Li, Y. Liu, and G.-Z. Ning, Light Doubly Charged Higgs Boson via the WW^* Channel at LHC, *Eur. Phys. J. C* **75**, 574 (2015), [arXiv:1404.5207 \[hep-ph\]](#).
- [41] S. Kanemura, M. Kikuchi, K. Yagyu, and H. Yokoya, Bounds on the mass of doubly-charged Higgs bosons in the same-sign diboson decay scenario, *Phys. Rev. D* **90**, 115018 (2014), [arXiv:1407.6547 \[hep-ph\]](#).
- [42] S. Kanemura, M. Kikuchi, H. Yokoya, and K. Yagyu, LHC Run-I constraint on the mass of doubly charged Higgs bosons in the same-sign diboson decay scenario, *PTEP* **2015**, 051B02 (2015), [arXiv:1412.7603 \[hep-ph\]](#).
- [43] Z.-L. Han, R. Ding, and Y. Liao, LHC Phenomenology of Type II Seesaw: Nondegenerate Case, *Phys. Rev. D* **91**, 093006 (2015), [arXiv:1502.05242 \[hep-ph\]](#).
- [44] Z.-L. Han, R. Ding, and Y. Liao, LHC phenomenology of the type II seesaw mechanism: Observability of neutral scalars in the nondegenerate case, *Phys. Rev. D* **92**, 033014 (2015), [arXiv:1506.08996 \[hep-ph\]](#).
- [45] D. Das and A. Santamaria, Updated scalar sector constraints in the Higgs triplet model, *Phys. Rev. D* **94**, 015015 (2016), [arXiv:1604.08099 \[hep-ph\]](#).
- [46] S. Blunier, G. Cottin, M. A. Díaz, and B. Koch, Phenomenology of a Higgs triplet model at future e^+e^- colliders, *Phys. Rev. D* **95**, 075038 (2017), [arXiv:1611.07896 \[hep-ph\]](#).
- [47] M. Mitra, S. Niyogi, and M. Spannowsky, Type-II Seesaw Model and Multilepton Signatures at Hadron Colliders, *Phys. Rev. D* **95**, 035042 (2017), [arXiv:1611.09594 \[hep-ph\]](#).
- [48] K. S. Babu and S. Jana, Probing Doubly Charged Higgs Bosons at the LHC through Photon Initiated Processes, *Phys. Rev. D* **95**, 055020 (2017), [arXiv:1612.09224 \[hep-ph\]](#).
- [49] T. Nomura, H. Okada, and H. Yokoya, Discriminating leptonic Yukawa interactions with doubly charged scalar at the ILC, *Nucl. Phys. B* **929**, 193 (2018), [arXiv:1702.03396 \[hep-ph\]](#).
- [50] P. S. B. Dev, C. M. Vila, and W. Rodejohann, Naturalness in testable type II seesaw scenarios, *Nucl. Phys. B* **921**, 436 (2017), [arXiv:1703.00828 \[hep-ph\]](#).
- [51] D. K. Ghosh, N. Ghosh, I. Saha, and A. Shaw, Revisiting the high-scale validity of the type II seesaw model with novel LHC signature, *Phys. Rev. D* **97**, 115022 (2018), [arXiv:1711.06062 \[hep-ph\]](#).
- [52] P. Agrawal, M. Mitra, S. Niyogi, S. Shil, and M. Spannowsky, Probing the Type-II Seesaw Mechanism through the Production of Higgs Bosons at a Lepton Collider, *Phys. Rev. D* **98**, 015024 (2018), [arXiv:1803.00677 \[hep-ph\]](#).
- [53] P. S. B. Dev, R. N. Mohapatra, and Y. Zhang, Probing TeV scale origin of neutrino mass at future lepton colliders via neutral and doubly-charged scalars, *Phys. Rev. D* **98**, 075028 (2018), [arXiv:1803.11167 \[hep-ph\]](#).
- [54] P. S. B. Dev, M. J. Ramsey-Musolf, and Y. Zhang, Doubly-Charged Scalars in the Type-II Seesaw Mechanism: Fundamental Symmetry Tests and High-Energy Searches, *Phys. Rev. D* **98**, 055013 (2018), [arXiv:1806.08499 \[hep-ph\]](#).
- [55] A. Crivellin, M. Ghezzi, L. Panizzi, G. M. Pruna, and A. Signer, Low- and high-energy phenomenology of a doubly charged scalar, *Phys. Rev. D* **99**, 035004 (2019), [arXiv:1807.10224 \[hep-ph\]](#).
- [56] P. S. B. Dev and Y. Zhang, Displaced vertex signatures of doubly charged scalars in the type-II seesaw and its left-right extensions, *JHEP* **10**, 199, [arXiv:1808.00943 \[hep-ph\]](#).
- [57] S. Antusch, O. Fischer, A. Hammad, and C. Scherb, Low scale type II seesaw: Present constraints and prospects for displaced vertex searches, *JHEP* **02**, 157, [arXiv:1811.03476 \[hep-ph\]](#).
- [58] P. S. B. Dev, S. Khan, M. Mitra, and S. K. Rai, Doubly-charged Higgs boson at a future electron-proton collider, *Phys. Rev. D* **99**, 115015 (2019), [arXiv:1903.01431 \[hep-ph\]](#).
- [59] R. Primulando, J. Julio, and P. Uttayarat, Scalar phenomenology in type-II seesaw model, *JHEP* **08**, 024, [arXiv:1903.02493 \[hep-ph\]](#).
- [60] T. B. de Melo, F. S. Queiroz, and Y. Villamizar, Doubly Charged Scalar at the High-Luminosity and High-Energy LHC, *Int. J. Mod. Phys. A* **34**, 1950157 (2019), [arXiv:1909.07429 \[hep-ph\]](#).

- [61] L. Rahili, A. Arhrib, and R. Benbrik, Associated production of SM Higgs with a photon in type-II seesaw models at the ILC, *Eur. Phys. J. C* **79**, 940 (2019), [arXiv:1909.07793 \[hep-ph\]](#).
- [62] R. Padhan, D. Das, M. Mitra, and A. Kumar Nayak, Probing doubly and singly charged Higgs bosons at the pp collider HE-LHC, *Phys. Rev. D* **101**, 075050 (2020), [arXiv:1909.10495 \[hep-ph\]](#).
- [63] E. J. Chun, S. Khan, S. Mandal, M. Mitra, and S. Shil, Same-sign tetralepton signature at the Large Hadron Collider and a future pp collider, *Phys. Rev. D* **101**, 075008 (2020), [arXiv:1911.00971 \[hep-ph\]](#).
- [64] B. Fuks, M. Nemevšek, and R. Ruiz, Doubly Charged Higgs Boson Production at Hadron Colliders, *Phys. Rev. D* **101**, 075022 (2020), [arXiv:1912.08975 \[hep-ph\]](#).
- [65] J. Gluza, M. Kordiaczynska, and T. Srivastava, Discriminating the HTM and MLRSM models in collider studies via doubly charged Higgs boson pair production and the subsequent leptonic decays, *Chin. Phys. C* **45**, 073113 (2021), [arXiv:2006.04610 \[hep-ph\]](#).
- [66] P. Bandyopadhyay, A. Karan, and C. Sen, Discerning Signatures of Seesaw Models and Complementarity of Leptonic Colliders, (2020), [arXiv:2011.04191 \[hep-ph\]](#).
- [67] X.-H. Yang and Z.-J. Yang, Doubly charged Higgs production at future ep colliders, *Chin. Phys. C* **46**, 063107 (2022), [arXiv:2103.11412 \[hep-ph\]](#).
- [68] S. Ashanujjaman and K. Ghosh, Revisiting type-II seesaw: present limits and future prospects at LHC, *JHEP* **03**, 195, [arXiv:2108.10952 \[hep-ph\]](#).
- [69] J. Heeck, W-boson mass in the triplet seesaw model, *Phys. Rev. D* **106**, 015004 (2022), [arXiv:2204.10274 \[hep-ph\]](#).
- [70] S. Ashanujjaman, K. Ghosh, and K. Huitu, Type-II seesaw: searching the LHC elusive low-mass triplet-like Higgses at e^-e^+ colliders, *Phys. Rev. D* **106**, 075028 (2022), [arXiv:2205.14983 \[hep-ph\]](#).
- [71] H. Bahl, W. H. Chiu, C. Gao, L.-T. Wang, and Y.-M. Zhong, Tripling down on the W boson mass, *Eur. Phys. J. C* **82**, 944 (2022), [arXiv:2207.04059 \[hep-ph\]](#).
- [72] Y. Cheng, X.-G. He, F. Huang, J. Sun, and Z.-P. Xing, Electroweak precision tests for triplet scalars, *Nucl. Phys. B* **989**, 116118 (2023), [arXiv:2208.06760 \[hep-ph\]](#).
- [73] J. Butterworth, J. Heeck, S. H. Jeon, O. Mattelaer, and R. Ruiz, Testing the scalar triplet solution to CDF's heavy W problem at the LHC, *Phys. Rev. D* **107**, 075020 (2023), [arXiv:2210.13496 \[hep-ph\]](#).
- [74] S. Ashanujjaman, K. Ghosh, and R. Sahu, Low-mass doubly charged Higgs bosons at the LHC, *Phys. Rev. D* **107**, 015018 (2023), [arXiv:2211.00632 \[hep-ph\]](#).
- [75] T. Li, C.-Y. Yao, and M. Yuan, Revealing the origin of neutrino masses through the Type II Seesaw mechanism at high-energy muon colliders, *JHEP* **03**, 137, [arXiv:2301.07274 \[hep-ph\]](#).
- [76] F. Xu, Neutral and doubly charged scalars at future lepton colliders, *Phys. Rev. D* **108**, 036002 (2023), [arXiv:2302.08653 \[hep-ph\]](#).
- [77] S. P. Maharathy and M. Mitra, Type-II see-saw at $\mu+\mu^-$ collider, *Phys. Lett. B* **844**, 138105 (2023), [arXiv:2304.08732 \[hep-ph\]](#).
- [78] S. Ashanujjaman and S. P. Maharathy, Probing compressed mass spectra in the type-II seesaw model at the LHC, *Phys. Rev. D* **107**, 115026 (2023), [arXiv:2305.06889 \[hep-ph\]](#).
- [79] K. Fridell, R. Kitano, and R. Takai, Lepton flavor physics at $\mu^+\mu^+$ colliders, *JHEP* **06**, 086, [arXiv:2304.14020 \[hep-ph\]](#).
- [80] G. Lichtenstein, M. A. Schmidt, G. Valencia, and R. R. Volkas, Complementarity of μ TRISTAN and Belle II in searches for charged-lepton flavour violation, *Phys. Lett. B* **845**, 138144 (2023), [arXiv:2307.11369 \[hep-ph\]](#).
- [81] P. S. B. Dev, J. Heeck, and A. Thapa, Neutrino mass models at μ TRISTAN, *Eur. Phys. J. C* **84**, 148 (2024), [arXiv:2309.06463 \[hep-ph\]](#).
- [82] J.-C. Jia, Z.-L. Han, F. Huang, Y. Jin, and H. Li, Production of single doubly charged Higgs bosons at muon colliders, *Phys. Rev. D* **111**, 015009 (2025), [arXiv:2409.16582 \[hep-ph\]](#).
- [83] O. A. Ducu, A. E. Dumitriu, A. Jinaru, R. Kukla, E. Monnier, G. Moultaqa, A. Tudorache, and H. Xu, Type-II Seesaw Higgs triplet productions and decays at the LHC, *JHEP* **06**, 020, [arXiv:2410.14830 \[hep-ph\]](#).
- [84] F. F. Deppisch, P. S. B. Dev, and A. Pilaftsis, Neutrinos and Collider Physics, *New J. Phys.* **17**, 075019 (2015), [arXiv:1502.06541 \[hep-ph\]](#).
- [85] Y. Cai, T. Han, T. Li, and R. Ruiz, Lepton Number Violation: Seesaw Models and Their Collider Tests, *Front. in Phys.* **6**, 40 (2018), [arXiv:1711.02180 \[hep-ph\]](#).
- [86] M. Kakizaki, Y. Ogura, and F. Shima, Lepton flavor violation in the triplet Higgs model, *Phys. Lett. B* **566**, 210 (2003), [arXiv:hep-ph/0304254](#).
- [87] A. G. Akeroyd, M. Aoki, and H. Sugiyama, Lepton Flavour Violating Decays $\tau \rightarrow \text{anti-l l}$ and $\mu \rightarrow e \gamma$ in the Higgs Triplet Model, *Phys. Rev. D* **79**, 113010 (2009), [arXiv:0904.3640 \[hep-ph\]](#).
- [88] D. N. Dinh, A. Ibarra, E. Molinaro, and S. T. Petcov, The $\mu - e$ Conversion in Nuclei, $\mu \rightarrow e \gamma$, $\mu \rightarrow 3e$ Decays and TeV Scale See-Saw Scenarios of Neutrino Mass Generation, *JHEP* **08**, 125, [Erratum: *JHEP* 09, 023 (2013)], [arXiv:1205.4671 \[hep-ph\]](#).
- [89] N. D. Barrie and S. T. Petcov, Lepton Flavour Violation tests of Type II Seesaw Leptogenesis, *JHEP* **01**, 001, [arXiv:2210.02110 \[hep-ph\]](#).
- [90] G. Abbiendi *et al.* (OPAL), Search for doubly charged Higgs bosons with the OPAL detector at LEP, *Phys. Lett. B* **526**, 221 (2002), [arXiv:hep-ex/0111059](#).
- [91] J. Abdallah *et al.* (DELPHI), Search for doubly charged Higgs bosons at LEP-2, *Phys. Lett. B* **552**, 127 (2003), [arXiv:hep-ex/0303026](#).
- [92] Search for charged Higgs bosons: Preliminary combined results using LEP data collected at energies up to 209-GeV, in *2001 Europhysics Conference on High Energy Physics* (2001) [arXiv:hep-ex/0107031](#).
- [93] G. Aad *et al.* (ATLAS), Search for anomalous production of prompt same-sign lepton pairs and pair-produced doubly charged Higgs bosons with $\sqrt{s} = 8$ TeV pp collisions using the ATLAS detector, *JHEP* **03**, 041, [arXiv:1412.0237 \[hep-ex\]](#).
- [94] M. Aaboud *et al.* (ATLAS), Search for doubly charged Higgs boson production in multi-lepton final states with the ATLAS detector using proton-proton collisions at $\sqrt{s} = 13$ TeV, *Eur. Phys. J. C* **78**, 199 (2018), [arXiv:1710.09748 \[hep-ex\]](#).
- [95] G. Aad *et al.* (ATLAS), Search for doubly charged Higgs boson production in multi-lepton final states using 139 fb $^{-1}$ of proton-proton collisions at $\sqrt{s} = 13$ TeV with the ATLAS detector, *Eur. Phys. J. C* **83**, 605 (2023), [arXiv:2211.07505 \[hep-ex\]](#).

- [96] A search for doubly-charged Higgs boson production in three and four lepton final states at $\sqrt{s} = 13$ TeV, CMS-PAS-HIG-16-036 (2017).
- [97] G. Aad *et al.* (ATLAS), Search for doubly and singly charged Higgs bosons decaying into vector bosons in multi-lepton final states with the ATLAS detector using proton-proton collisions at $\sqrt{s} = 13$ TeV, *JHEP* **06**, 146, [arXiv:2101.11961 \[hep-ex\]](#).
- [98] G. Lichtenstein, M. A. Schmidt, G. Valencia, and R. R. Volkas, Z and Higgs boson decays with doubly-charged scalars at one-loop: Current constraints, future sensitivities, and application to lepton-triality models, *Nucl. Phys. B* **1013**, 116850 (2025), [arXiv:2312.09409 \[hep-ph\]](#).
- [99] G. Aad *et al.* (ATLAS, CMS), Measurements of the Higgs boson production and decay rates and constraints on its couplings from a combined ATLAS and CMS analysis of the LHC pp collision data at $\sqrt{s} = 7$ and 8 TeV, *JHEP* **08**, 045, [arXiv:1606.02266 \[hep-ex\]](#).
- [100] A. Tumasyan *et al.* (CMS), A portrait of the Higgs boson by the CMS experiment ten years after the discovery., *Nature* **607**, 60 (2022), [Erratum: *Nature* 623, (2023)], [arXiv:2207.00043 \[hep-ex\]](#).
- [101] G. Aad *et al.* (ATLAS), A detailed map of Higgs boson interactions by the ATLAS experiment ten years after the discovery, *Nature* **607**, 52 (2022), [Erratum: *Nature* 612, E24 (2022)], [arXiv:2207.00092 \[hep-ex\]](#).
- [102] A. M. Sirunyan *et al.* (CMS), Measurements of Higgs boson production cross sections and couplings in the diphoton decay channel at $\sqrt{s} = 13$ TeV, *JHEP* **07**, 027, [arXiv:2103.06956 \[hep-ex\]](#).
- [103] G. Aad *et al.* (ATLAS), Measurement of the properties of Higgs boson production at $\sqrt{s} = 13$ TeV in the $H \rightarrow \gamma\gamma$ channel using 139 fb⁻¹ of *pp* collision data with the ATLAS experiment, *JHEP* **07**, 088, [arXiv:2207.00348 \[hep-ex\]](#).
- [104] Y. Heo, D.-W. Jung, and J. S. Lee, Higgs boson precision analysis of the full LHC run 1 and run 2 data, *Phys. Rev. D* **110**, 013003 (2024), [arXiv:2402.02822 \[hep-ph\]](#).
- [105] M. Cepeda *et al.*, Report from Working Group 2: Higgs Physics at the HL-LHC and HE-LHC, *CERN Yellow Rep. Monogr.* **7**, 221 (2019), [arXiv:1902.00134 \[hep-ph\]](#).
- [106] M. Dong *et al.* (CEPC Study Group), CEPC Conceptual Design Report: Volume 2 - Physics & Detector, (2018), [arXiv:1811.10545 \[hep-ex\]](#).
- [107] A. Abada *et al.* (FCC), FCC Physics Opportunities: Future Circular Collider Conceptual Design Report Volume 1, *Eur. Phys. J. C* **79**, 474 (2019).
- [108] C. Accettura *et al.*, Towards a muon collider, *Eur. Phys. J. C* **83**, 864 (2023), [Erratum: *Eur.Phys.J.C* 84, 36 (2024)], [arXiv:2303.08533 \[physics.acc-ph\]](#).
- [109] J. de Blas *et al.*, Higgs Boson Studies at Future Particle Colliders, *JHEP* **01**, 139, [arXiv:1905.03764 \[hep-ph\]](#).
- [110] L. Castelli, Higgs Physics at the Muon Collider, *Particles* **8**, 28 (2025).
- [111] L. Lavoura and L.-F. Li, Making the small oblique parameters large, *Phys. Rev. D* **49**, 1409 (1994), [arXiv:hep-ph/9309262](#).
- [112] S. Kanemura and K. Yagyu, Radiative corrections to electroweak parameters in the Higgs triplet model and implication with the recent Higgs boson searches, *Phys. Rev. D* **85**, 115009 (2012), [arXiv:1201.6287 \[hep-ph\]](#).
- [113] S. Navas *et al.* (Particle Data Group), Review of particle physics, *Phys. Rev. D* **110**, 030001 (2024).
- [114] G. Aad *et al.* (ATLAS), Measurement of the W-boson mass and width with the ATLAS detector using proton-proton collisions at $\sqrt{s} = 7$ TeV, *Eur. Phys. J. C* **84**, 1309 (2024), [arXiv:2403.15085 \[hep-ex\]](#).
- [115] V. Chekhovsky *et al.* (CMS), High-precision measurement of the W boson mass with the CMS experiment at the LHC, (2024), [arXiv:2412.13872 \[hep-ex\]](#).
- [116] T. Aaltonen *et al.* (CDF), High-precision measurement of the W boson mass with the CDF II detector, *Science* **376**, 170 (2022).
- [117] D. de Florian *et al.* (LHC Higgs Cross Section Working Group), Handbook of LHC Higgs Cross Sections: 4. Deciphering the Nature of the Higgs Sector, *CERN Yellow Rep. Monogr.* **2**, 1 (2017), [arXiv:1610.07922 \[hep-ph\]](#).
- [118] M. A. Shifman, A. I. Vainshtein, M. B. Voloshin, and V. I. Zakharov, Low-Energy Theorems for Higgs Boson Couplings to Photons, *Sov. J. Nucl. Phys.* **30**, 711 (1979).
- [119] C.-S. Chen, C.-Q. Geng, D. Huang, and L.-H. Tsai, New Scalar Contributions to $h \rightarrow Z\gamma$, *Phys. Rev. D* **87**, 075019 (2013), [arXiv:1301.4694 \[hep-ph\]](#).
- [120] C.-S. Chen, C.-Q. Geng, D. Huang, and L.-H. Tsai, $h \rightarrow Z\gamma$ in Type-II seesaw neutrino model, *Phys. Lett. B* **723**, 156 (2013), [arXiv:1302.0502 \[hep-ph\]](#).
- [121] G. Aad *et al.* (ATLAS, CMS), Evidence for the Higgs Boson Decay to a Z Boson and a Photon at the LHC, *Phys. Rev. Lett.* **132**, 021803 (2024), [arXiv:2309.03501 \[hep-ex\]](#).

Supplemental Material

A. EXPRESSIONS FOR THE OBLIQUE PARAMETERS S , T AND U

To a good approximation, neglecting the effects of scalar mixing, the oblique parameters S , T , and U are given by [111]:³

$$S = -\frac{1}{3\pi} \ln \frac{m_{H^{\pm\pm}}^2}{m_{H^0}^2} - \frac{2}{\pi} \left[(1 - 2s_W^2)^2 \xi \left(\frac{m_{H^{\pm\pm}}^2}{m_Z^2}, \frac{m_{H^{\pm\pm}}^2}{m_Z^2} \right) + s_W^4 \xi \left(\frac{m_{H^\pm}^2}{m_Z^2}, \frac{m_{H^\pm}^2}{m_Z^2} \right) + \xi \left(\frac{m_{H^0}^2}{m_Z^2}, \frac{m_{H^0}^2}{m_Z^2} \right) \right], \quad (\text{S1})$$

$$T = \frac{1}{8\pi c_W^2 s_W^2} \left[\eta \left(\frac{m_{H^{\pm\pm}}^2}{m_Z^2}, \frac{m_{H^\pm}^2}{m_Z^2} \right) + \eta \left(\frac{m_{H^\pm}^2}{m_Z^2}, \frac{m_{H^0}^2}{m_Z^2} \right) \right], \quad (\text{S2})$$

$$U = \frac{1}{6\pi} \ln \frac{m_{H^\pm}^4}{m_{H^{\pm\pm}}^2 m_{H^0}^2} + \frac{2}{\pi} \left[(1 - 2s_W^2)^2 \xi \left(\frac{m_{H^{\pm\pm}}^2}{m_Z^2}, \frac{m_{H^{\pm\pm}}^2}{m_Z^2} \right) + s_W^4 \xi \left(\frac{m_{H^\pm}^2}{m_Z^2}, \frac{m_{H^\pm}^2}{m_Z^2} \right) + \xi \left(\frac{m_{H^0}^2}{m_Z^2}, \frac{m_{H^0}^2}{m_Z^2} \right) \right] \\ - \frac{2}{\pi} \left[\xi \left(\frac{m_{H^{\pm\pm}}^2}{m_W^2}, \frac{m_{H^\pm}^2}{m_W^2} \right) + \xi \left(\frac{m_{H^\pm}^2}{m_W^2}, \frac{m_{H^0}^2}{m_W^2} \right) \right], \quad (\text{S3})$$

where the functions are defined as

$$\xi(x, y) = \frac{4}{9} - \frac{5}{12}(x+y) + \frac{1}{6}(x-y)^2 + \frac{1}{4} \left[x^2 - y^2 - \frac{1}{3}(x-y)^3 - \frac{x^2 + y^2}{x-y} \right] \ln \frac{x}{y} - \frac{1}{12} d(x, y) f(x, y), \quad (\text{S4})$$

$$\eta(x, y) = x + y - \frac{2xy}{x-y} \ln \frac{x}{y}, \quad (\text{S5})$$

$$d(x, y) = -1 + 2(x+y) - (x-y)^2, \quad (\text{S6})$$

$$f(x, y) = \begin{cases} -2\sqrt{d(x, y)} \left\{ \arctan \left[\frac{x-y+1}{\sqrt{d(x, y)}} \right] - \arctan \left[\frac{x-y-1}{\sqrt{d(x, y)}} \right] \right\} & d(x, y) > 0 \\ \sqrt{-d(x, y)} \ln \left[\frac{x+y-1+\sqrt{-d(x, y)}}{x+y-1-\sqrt{-d(x, y)}} \right] & d(x, y) \leq 0 \end{cases}. \quad (\text{S7})$$

B. RELEVANT LOOP FUNCTIONS IN THE LOOP-INDUCED HIGGS DECAYS $h \rightarrow \gamma\gamma$ AND $h \rightarrow Z\gamma$

A. $h \rightarrow \gamma\gamma$

The loop-induced $h \rightarrow \gamma\gamma$ decay rate in the SM and in the type-II seesaw model are respectively given by

$$\Gamma_{h \rightarrow \gamma\gamma}^{(\text{SM})} = \frac{\alpha_{\text{em}}^2 G_F m_h^3}{128\sqrt{2}\pi^3} \left| g_{h\gamma\gamma}^{(\text{SM})} \right|^2, \quad (\text{S8})$$

where the effective couplings $g_{h\gamma\gamma}^{(\text{SM})}$ are given by [33, 36, 118]

$$g_{h\gamma\gamma}^{\text{SM}} = \sum_f N_f^c Q_f^2 \beta_{\gamma\gamma}^{1/2}(r_f) + \beta_{\gamma\gamma}^1(r_W), \quad (\text{S9})$$

$$g_{h\gamma\gamma} = \sum_f N_f^c Q_f^2 g_{ff}^h \beta_{\gamma\gamma}^{1/2}(r_f) + g_{WW}^h \beta_{\gamma\gamma}^1(r_W) + \frac{\lambda_{hH^+H^-} v_\Phi}{2m_{H^\pm}^2} \beta_{\gamma\gamma}^0(r_{H^\pm}) + 4 \frac{\lambda_{hH^{++}H^{--}} v_\Phi}{2m_{H^{\pm\pm}}^2} \beta_{\gamma\gamma}^0(r_{H^{\pm\pm}}). \quad (\text{S10})$$

Here Q_f (I_{3f}) is the electric charge (third component of the weak isospin) of the SM fermion f running in the loop, N_f^c is the color factor (3 for quarks, and 1 for leptons), $r_X = 4m_X^2/m_h^2$, and the loop functions $\beta_{\gamma\gamma}^{0,1/2,1}$ are collected

³ In Eq. (4.1) of Ref. [33], the second loop function in the square brackets $\xi \left(m_{T_3}^2/m_W^2, m_{T_3}^2/m_W^2 \right)$, appearing in the

expression for the parameter U , should be corrected to $\xi \left(m_{T_3}^2/m_W^2, m_{T_3-1}^2/m_W^2 \right)$.

below:

$$\beta_{\gamma\gamma}^0(x) = -x[1 - xf(x)] , \quad (\text{S11})$$

$$\beta_{\gamma\gamma}^{1/2}(x) = 2x[1 + (1-x)f(x)] , \quad (\text{S12})$$

$$\beta_{\gamma\gamma}^1(x) = -[2 + 3x + 3x(2-x)f(x)] , \quad (\text{S13})$$

with the function $f(x)$ defined as

$$f(x) = \begin{cases} \left[\sin^{-1}(\sqrt{1/x}) \right]^2 & x \geq 1 \\ -\frac{1}{4} \left[\log \frac{1 + \sqrt{1-x}}{1 - \sqrt{1-x}} - i\pi \right]^2 & x < 1 \end{cases} . \quad (\text{S14})$$

The trilinear couplings $\lambda_{hH^+H^-}$ and $\lambda_{hH^{++}H^{--}}$ are given by

$$\lambda_{hH^+H^-} = \cos \alpha \left\{ \frac{\lambda v_\Phi}{2} \sin^2 \beta + \left(\mu - \frac{\lambda_4 v_\Delta}{2\sqrt{2}} \right) \sin 2\beta + \left(\lambda_1 + \frac{\lambda_4}{2} \right) v_\Phi \cos^2 \beta \right\} \\ + \sin \alpha \left\{ \lambda_1 v_\Delta \sin^2 \beta + 2(\lambda_2 + \lambda_3) v_\Delta \cos^2 \beta - \frac{\lambda_4 v_\Phi}{2\sqrt{2}} \sin 2\beta \right\}, \quad (\text{S15})$$

$$\lambda_{hH^{++}H^{--}} = \lambda_1 v_\Phi \cos \alpha + 2\lambda_2 v_\Delta \sin \alpha , \quad (\text{S16})$$

where $\beta = \tan^{-1}(\sqrt{2}v_\Delta/v_\Phi)$ denotes the mixing angle between singly-charged states Φ^\pm and Δ^\pm .

B. $h \rightarrow Z\gamma$

Similarly, the loop-induced $h \rightarrow Z\gamma$ decay rate is given by [36, 119]

$$\Gamma_{h \rightarrow Z\gamma}^{(\text{SM})} = \frac{\alpha_{\text{em}} G_F^2 m_W^2 m_h^3}{64\pi^4} \left(1 - \frac{m_Z^2}{m_h^2} \right)^3 \left| g_{hZ\gamma}^{(\text{SM})} \right|^2 , \quad (\text{S17})$$

where the effective couplings are given by

$$g_{hZ\gamma}^{\text{SM}} = \sum_f \frac{2N_f^c}{\cos \theta_w} Q_f (I_{3f} - 2Q_f \sin^2 \theta_w) \beta_{Z\gamma}^{1/2}(r_f, z_f) + \beta_{Z\gamma}^1(r_W, z_W) , \quad (\text{S18})$$

$$g_{hZ\gamma} = \sum_f \frac{2N_f^c}{\cos \theta_w} Q_f (I_{3f} - 2Q_f \sin^2 \theta_w) g_{ff}^h \beta_{Z\gamma}^{1/2}(r_f, z_f) + g_{WW}^h \beta_{Z\gamma}^1(r_W, z_W) \\ - g_{ZH^+H^-} \frac{\lambda_{hH^+H^-} v}{2m_{H^\pm}^2} \beta_{Z\gamma}^0(r_{H^\pm}, z_{H^\pm}) - 2g_{ZH^{++}H^{--}} \frac{\lambda_{hH^{++}H^{--}} v}{2m_{H^{\pm\pm}}^2} \beta_{Z\gamma}^0(r_{H^{\pm\pm}}, z_{H^{\pm\pm}}) , \quad (\text{S19})$$

with

$$g_{ZH^+H^-} = \sin^2 \beta - \frac{2 \sin^2 \theta_w}{\cos 2\theta_w} \cos^2 \beta , \quad g_{ZH^{++}H^{--}} = 2 . \quad (\text{S20})$$

The loop functions $\beta_{Z\gamma}^{0,1/2,1}$ are given by

$$\beta_{Z\gamma}^0(x, y) = \frac{\cos 2\theta_w}{\cos \theta_w} I_1(x, y) , \quad (\text{S21})$$

$$\beta_{Z\gamma}^{1/2}(x, y) = I_1(x, y) - I_2(x, y) , \quad (\text{S22})$$

$$\beta_{Z\gamma}^1(x, y) = \cos \theta_w \left\{ \left(1 + \frac{2}{x} \right) \tan^2 \theta_w - \left(5 + \frac{2}{x} \right) \right\} I_1(x, y) + 4 \cos \theta_w (3 - \tan^2 \theta_w) I_2(x, y) . \quad (\text{S23})$$

with the functions $I_{1,2}(x, y)$ defined as

$$I_1(x, y) = \frac{xy}{2(x-y)} + \frac{x^2y^2}{2(x-y)^2} [f(x) - f(y)] + \frac{x^2y}{(x-y)^2} [j(x) - j(y)], \quad (\text{S24})$$

$$I_2(x, y) = -\frac{xy}{2(x-y)} [f(x) - f(y)], \quad (\text{S25})$$

with

$$j(x) = \begin{cases} \sqrt{x-1} \sin^{-1}(\sqrt{1/x}) & x \geq 1 \\ \frac{1}{2}\sqrt{1-x} \left[\log \frac{1+\sqrt{1-x}}{1-\sqrt{1-x}} - i\pi \right] & x < 1 \end{cases}. \quad (\text{S26})$$